

Simulation of fatigue crack paths using a continuous dislocation distribution formulation

P. Hansson¹, S. Melin² and C. Persson³

¹ Division of Mechanics, Lund Institute of Technology, Box 118, SE-22100 Lund, Per.Hansson@mek.lth.se

² Solveig.Melin@mek.lth.se

³ Division of Materials, Christer.Persson@material.lth.se

***ABSTRACT.** When subjected to fatigue loading microstructurally short cracks grow in a zigzag shape in a single shear mechanism due to nucleation, gliding and annihilation of dislocations. Such crack shapes are computationally time consuming due to the scale of refinement needed in a numerical model. Therefore an investigation of to what extent a zigzag geometry could be simplified, keeping acceptable accuracy as regards geometry dependent parameters, was performed. It was found that using a model correctly describing the zigzag section closest to the crack tip only, ignoring all zigzag sections between this last one and the initial crack tip, very good agreement was obtained, both when calculating the nucleation stress for dislocations and the resolved shear stress in front of the crack.*

INTRODUCTION

It is well known that fatigue growth of microstructurally short cracks is influenced by the surrounding microstructure of the material, such as grain boundaries, slip plane orientation and local plasticity in the crack tip region. Such short cracks grow in a single shear mechanism, cf. Suresh [1], due to nucleation and gliding of dislocations, creating a zigzag shaped crack. For short cracks and low growth rates it is important to account for individual dislocations created during the fatigue process. Models taking this into account have been developed by Riemelmoser et. al. [2] to study the cyclic crack tip plasticity for a long mode I crack, and by Bjerken and Melin [3] to study the influence of grain boundaries on a short mode I fatigue crack. A similar approach was used by Krupp et. al. [4], describing the plasticity with dislocation dipole elements, to study the growth of a short crack in a duplex steel.

In this study, two models simplifying the complex geometry emerging during fatigue growth of short cracks have been developed and compared to the correct crack shape as regards dislocation nucleation stress and shear stress in front of the crack along different slip planes.

PROBLEM FORMULATION

The investigation involves a microstructurally short edge crack situated within one grain in a semi-infinite body. The initially straight crack is inclined at an angle α to the normal of the free edge and the external load σ_{yy}^{∞} is applied parallel to this free edge, cf. Fig. 1.1. Within the grain slip planes along which dislocations can nucleate and thus creating a plastic zone are separated by an angle β . A grain boundary, parallel with the free edge, is introduced a certain distance in front of the initial crack tip, acting as a dislocation barrier, preventing the plasticity to spread into the next grain.

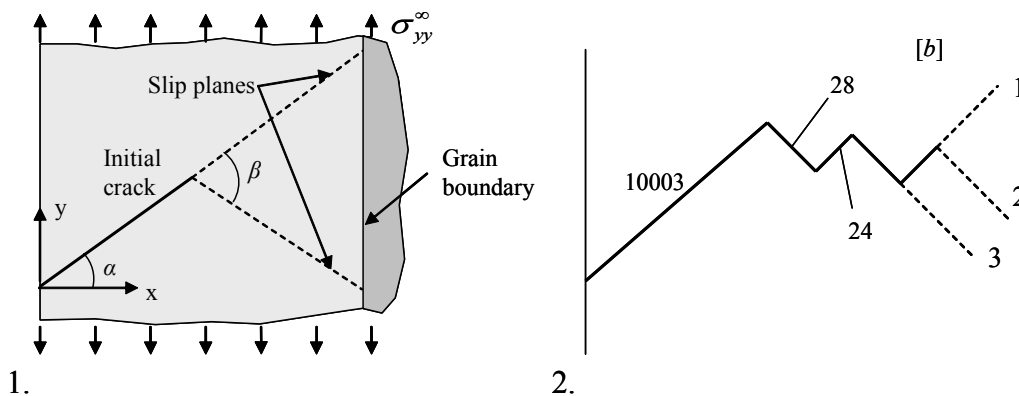


Figure 1. 1. Initial geometry of the short edge crack. 2. Resulting crack shape consisting of five crack segments with three marked slip planes; all lengths expressed in terms of Burgers vector, b .

When the initial, straight crack is subjected to fatigue loading, the crack grows, forming a zigzag shaped crack, cf Fig. 1.2. Such a zigzag shaped crack is time consuming and difficult to model due to the large number of elements needed to capture all stress concentrations at the corner points and at the crack tip. Therefore, attempts to simplify the crack geometry and thereby reduce the number of elements needed to capture the crack development was made. Two different models were created and compared with the correct crack shape, schematically shown in Fig. 2.1, obtained by the distributed dipole element approach described below. In the first simplified model, the crack consisted of four crack segments, with the two segments closest to the crack tip identical to the correct crack shape, cf. Fig. 2.2. In the second, the crack was assumed to consist of three crack segments only, with the segment closest to the crack tip identical to the correct crack shape, cf. Fig. 2.3.

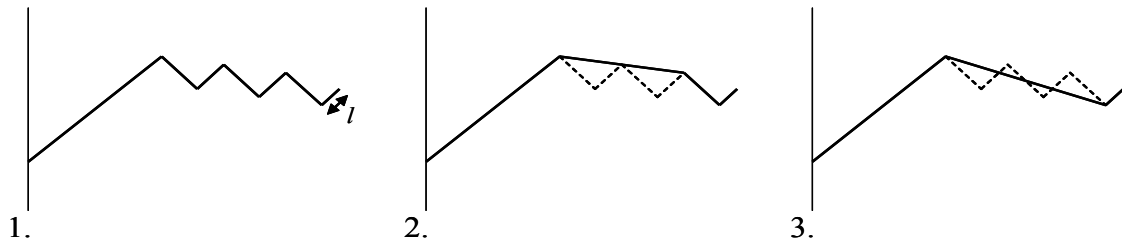


Figure 2. Crack shapes of the three models; the correct crack shape is seen as a dashed line. 1. The correct crack shape. 2. Crack shape consisting of four crack segments. 3. Crack shape consisting of three crack segments.

DISTRIBUTED DIPOLE ELEMENT APPROACH

In this study both the external boundary, defined as the free edge together with the crack, and the plasticity along the slip planes are described with dislocation dipole elements in the spirit of a boundary element approach, cf. Hansson and Melin [5]. Only plane problems are addressed and, therefore, only edge dislocations are needed in the formulation. The dislocation dipole elements along the external boundary consists of four dislocations, cf. Fig. 3.1, two glide dislocations, grey in Fig. 3.1, and two climb dislocations, black in Fig. 3.1. Using both types of dislocations makes it possible to determine both the shape of the free edge and the opening and the shearing between the crack surfaces. The elements describing the plasticity along the slip planes only consists of two glide dislocations, cf. Fig. 3.2, because only shearing of the surfaces is allowed along the slip planes. The two dislocations of same type constituting an element have the same size but opposite direction of their Burgers vectors.

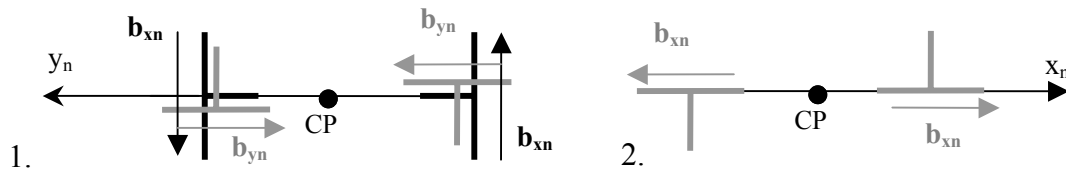


Figure 3. Dislocation dipole elements: 1. along the external boundary and 2. along the slip planes.

Stress calculation

The stresses at an arbitrary point within the body are calculated as the sum of the stress contributions from all dislocations in the dipole elements and the applied load. The sizes of the dislocations forming the dipole elements are calculated from an equilibrium equation, describing the normal and shear stresses along the external boundary and the shear stresses along the slip planes. Knowing that the normal and shear stress along the external boundary must equal zero and that the shear stress along a slip planes cannot exceed the lattice resistance of the material, the magnitudes of the dislocations of all dipole elements can be determined. A more detailed description of the procedure of solving of the equilibrium equation and the stress calculation is found in [5].

Nucleation condition

It is assumed that the only sources of dislocation nucleation are the crack tip and eventual corner points of the crack. The dislocations nucleate in pairs, consisting of two dislocations of the same size but of opposite sign, separated a small distance r_{nuc} . Such a pair nucleates when the resolved shear stress, τ_{slip} , exceeds a critical value τ_{nuc} , according to Eq. (1), at the distance r_{nuc} in front of the crack. Thus, the condition for nucleation is:

$$\tau_{slip}(\theta) = \frac{\sigma_{yy} - \sigma_{xx}}{2} \sin 2\theta + \sigma_{xy} \cos 2\theta \geq \tau_{nuc} \quad (1)$$

where θ is the angle between the global x -axis and the slip plane in focus, and σ_{xx} , σ_{yy} and σ_{xy} are the stresses at the nucleation point. The nucleation stress is found by a balance consideration between the two dislocations, and varies with crack geometry. The nucleation condition used here is described in more detail in [6], by Hansson and Melin.

Plastic zone

The plastic zone is modelled by dislocation dipole elements placed along specific slip planes in the material. In the crack tip vicinity the resolved shear stress exceeds the lattice resistance of the material, resulting in a dislocation free zone. In this dislocation free zone no dipole elements are placed, cf Fig. 4, and at the end points of this zone two glide dislocations of opposite signs, each of size nb , are placed, where n is the number of dislocations nucleated along this specific slip plane.

At the beginning of the first load cycle it is assumed that no dislocations exist within the material. When the resolved shear stress along a slip plane in front of the crack gets sufficiently high a dislocation pair is nucleated along this slip plane, resulting in $n=1$ and increasing the size of the dipole elements in the plastic zone. The stress in front of the crack is recalculated, now including the newly nucleated dislocations. If the nucleation stress still is exceeded, another dislocation is nucleated and n is updated to $n=2$. This nucleation process along all possible slip planes continues until the stresses in front of the crack falls below the nucleation stress and unloading starts. During unloading some of the dislocations are forced to annihilate, causing crack growth. Thereafter a new load cycle begins and the new nucleation stresses are calculated, followed by eventual dislocation nucleation and annihilation. A more detailed description of the nucleation and annihilation process during the loading cycle is found in [5].

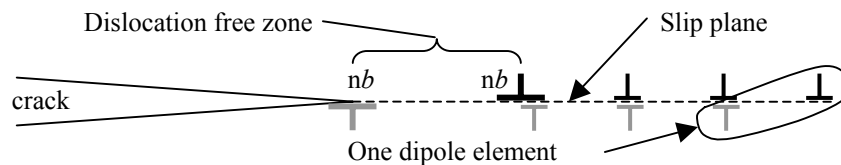


Figure 4. Description of modelling the plastic zone along a slip plane.

RESULTS AND DISCUSSION

Initial conditions

The material modelled in this study is pure iron, which has a bcc crystal structure. The material parameters are listed in Table 1, cf. Askeland [7], together with the initial geometrical parameters seen in Fig. 1.1. The choice of angle between the slip planes depends on the crystal structure and orientation of the bcc material and is discussed in detail in [6].

Table 1. Material properties and initial geometrical parameters.

Shear modulus, μ	80GPa	Initial crack length, a_0	10000 b
Poisson's ratio, ν	0.3	Crack angle, α	35.3°
Burgers vector, b	0.25 nm	Angle between slip planes, β	70.6°
Lattice resistance, τ_{crit}	40MPa	Distance to grain boundary, l_{GB}	10000 b
		Applied load, $\sigma_{yy\max}^\infty, \sigma_{yy\min}^\infty$	220, 20 MPa

With the chosen initial conditions of Table 1 a crack will develop according to Fig. 1.2, with lengths expressed in terms of Burgers vectors. It was found that the crack grew approximately the same distance along the upper slip planes, about $24b$, and similarly approximately $28b$ along the lower ones. The creation of one zigzag section, consisting of one crack segment along the lower slip plane of $28b$ length, and one crack segment along the upper slip plane of $24b$ of length, results after seven load cycles. In this investigation, it is assumed that the growth pattern is built from such zigzag sections that emerge when a longer crack is created during further load cycles.

Comparison of the nucleation stresses

The first investigation is aimed at evaluating the differences between the three models regarding the nucleation stress at all possible nucleation sites. This calculation was performed for different crack lengths, i.e. numbers of crack segments, with two different lengths of the last crack segment closest to the crack tip, $l=6b$ and $l=16b$, cf. Fig. 2.1. The nucleation stress τ_{nuc} as function of number of crack segments for the three models are shown in Fig. 5 at the three possible nucleation points, a distance r_{nuc} from the crack tip and corner point closest to the crack tip along slip planes 1, 2 and 3, cf. Fig. 1.2. The choice of r_{nuc} is discussed in [6].

In Fig. 5.1 the nucleation stress along plane 1 in Fig. 1.2 is seen for the three models as functions of number of crack segments constituting the correct crack shape. It is found that the model with three crack segments shows much less agreement with the correct model than the model with four crack segments. It is also seen that the differences between the models increases with increasing number of crack segments and that the difference is larger when $l=6b$ than when $l=16b$. In Figs. 5.2 and 5.3 the nucleation stresses along plane 2 in Fig. 1.2 is seen, with Fig. 5.3 being an enlargement of the curves with $l=16b$. In this case, the differences between the models are much smaller than in along plane 1. However, the model with four crack segments is also in

this case somewhat more correct than the model with three crack segments. The nucleation stress along plane 3 from Fig. 1.2 is seen in Fig. 5.4. Only the results for the shorter last segment of the crack is presented because when this last segment is longer, as in the case $l = 16b$, no nucleation occurs along slip plane 3. Also in this case the model with four crack segments is in better agreement with the correct model than the model with three segments, but a larger difference between the correct values and the ones obtained by the model with four crack segments was observed along this slip plane than along planes 1 and 2.

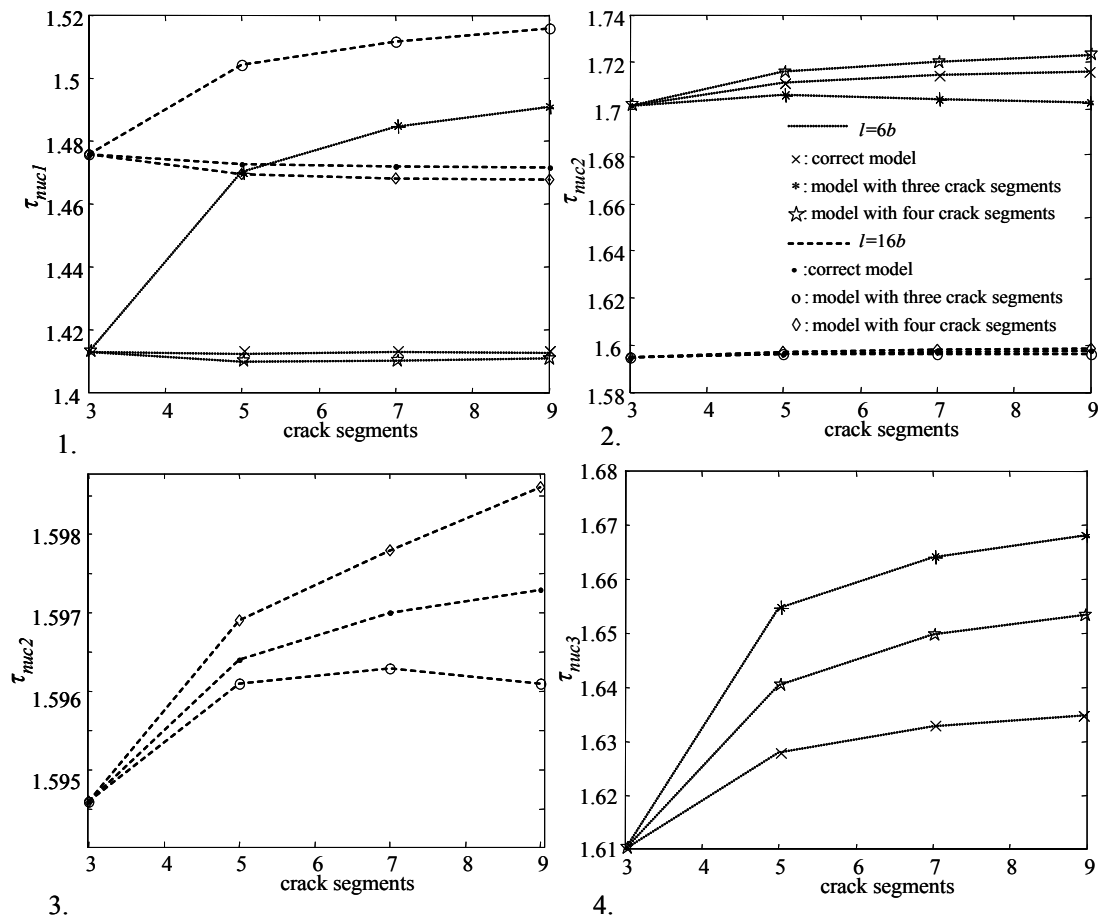


Figure 5. Nucleation stress, τ_{nuc} , as function of number of crack segments of the correct crack shape for the three different models for two different lengths, l , of the last crack segment.

In all investigated cases, the model with four crack segments is more correct than the model with only three segments. Both simplified models showed better agreement with the correct model with a longer last segment of the crack due to the increased distance from the simplified area. The simplified models showed an increasing error with increasing number of crack segments, especially the model with three crack segments. This outcome is expected since the simplifications reduce the number of stress

concentrations in terms of corner points, and the effect of this strikes plane 3, being closest to the simplified area, the worst. It is also expected that a longer last segment l reduce the effects of the simplifications since the stress concentration at the crack tip gets further away from the simplified area.

Comparison of the resolved shear stresses

In the second part of the comparison between the three models, an analysis of the resolved shear stress at the nucleation points in front of the crack at maximum load was performed. The stresses were calculated along the same three planes at the possible nucleation positions, corresponding to the first investigation, and the results are seen in Fig. 6.

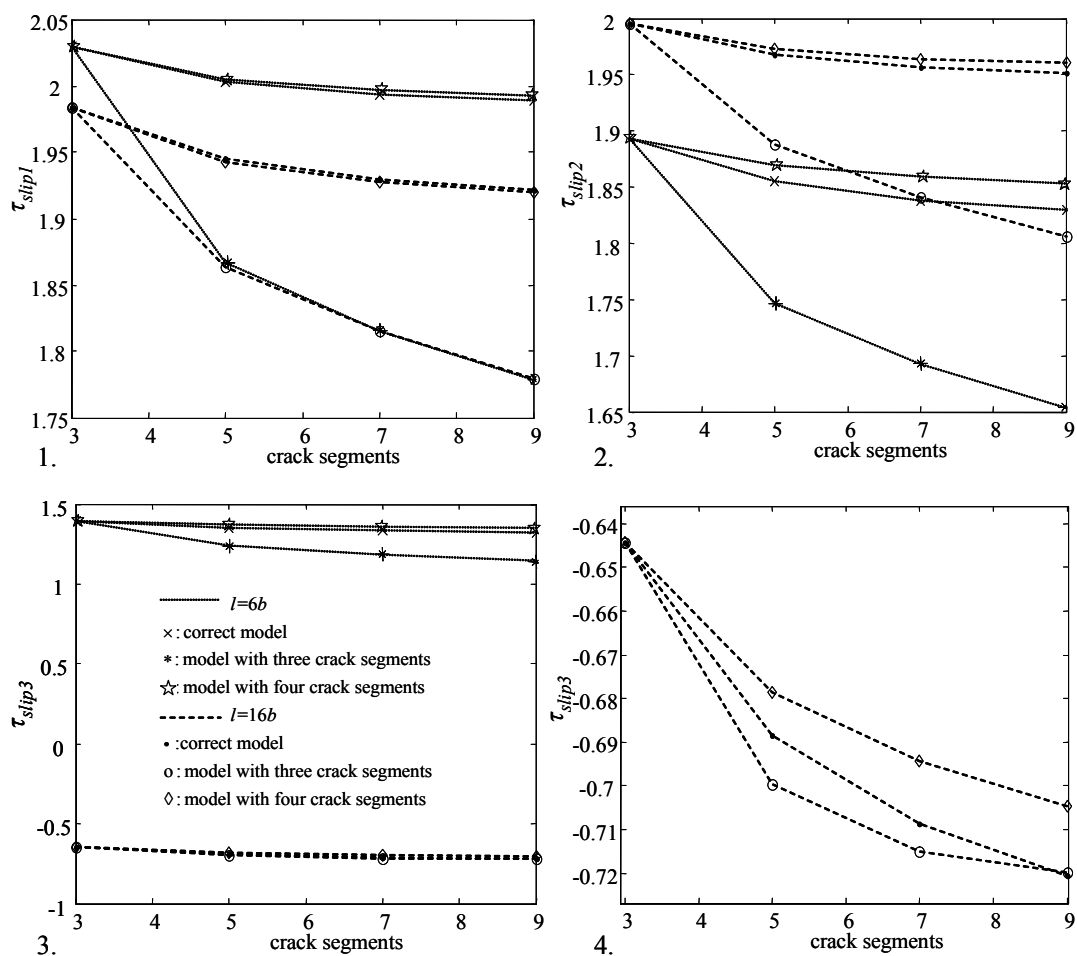


Figure 6. Nucleation stress, τ_{slip} , as function of number of crack segments for the three different models for two different lengths, l , of the last crack segment.

In Fig. 6.1 the resolved shear stress, τ_{slip} , is calculated along plane 1 in Fig. 1.2 as function of the number of crack segments describing the crack. It is seen that the model with four crack segments shows excellent agreement with the values from the correct

model for both lengths of the crack segment closest to the crack tip. The model with three crack segments, however, differs significantly from the correct values, especially when the last crack segment is short. In Fig. 6.2 the resolved shear stress along plane 2 is shown. It can be seen that also here the model with four crack segments shows good agreement with the correct values. However, the discrepancy was somewhat larger than along the upper slip plane for both simplified models. The resolved shear stress for plane 3 is seen in Figs. 6.3 and 6.4, with Fig. 6.4 an enlargement of Fig. 6.3. The resolved shear stress is positive when the last segment of the crack is short and negative when this segment gets longer. Along this slip plane the difference between the models is small when the last segment of the crack is long but relatively large, as compared to the other slip planes, when the last segment of the crack is short.

Also when calculating the resolved shear stress, the model with four crack segments is more accurate than the model with three crack segments. The same trend as observed when studying the nucleation stress; an increase in length of the last segment of the crack gives more accurate results, applies also in this case, and the simplified models give the most accurate results along the upper slip plane. It was also observed that an increase in number of crack segments of the correct crack results in lowered shear stress in front of the crack. This is because the stress field induced by the corners of the crack shields the crack tip and lowers the stresses. The same effect, that the stress intensity factor is reduced after kinking, has been found by Melin [8].

CONCLUSIONS

It was found that a simplification of a zigzag shaped short crack through modelling the crack by its initial, straight configuration connected with the two last crack segments by a straight crack segment satisfactorily predicts nucleation stress as well as resolved shear stress in front of the crack. This significantly reduces the computational efforts and makes it possible to follow the crack growth during a large number of load cycles, enabling growth through several grains.

REFERENCES

1. Suresh, S. (1998), *Fatigue of Materials*, sec edition. University Press, Cambridge.
2. Riemelmoser F.O., Pippin R., Kolednik O. (1997) *Comp. Mech.*, 20, pp. 139-144.
3. Bjerken C., Melin S., (2004), *Engineering Fracture Mech.*, 71(15), pp. 2215-2227.
4. Krupp U., Düber, O., Christ, H.-J. and Künkler, B, (2003), *J. of Microscopy.*,13(3), pp. 313-320.
5. Hansson, P., Melin, S. and Persson, C., ECF 16, July 3-7, 2006.
6. Hansson, P., Melin, S. *Int. J. of Fatigue*. Accepted for publication 26/9-05.
7. Askeland D.R.,(1998) *The Science and Eng. of Materials*, third edition. Stanley Thornes (Publishers) Ltd.
8. Melin, S. (1994). *J. of Applied Mech.*, vol. 61, pp. 467-470.